**TAL
TECH**

TALLINN UNIVERSITY OF TECHNOLOGY
SCHOOL OF ENGINEERING
Department of Materials and Environmental Technology

Sb_2S_3 THIN FILMS FROM AN ALTERNATIVE METAL ORGANIC PRECURSOR BY ULTRASONIC SPRAY PYROLYSIS

ALTERNATIIVSEST METALLORGAANILISEST LÄHTEAINEST ULTRAHELIPIHUSTUSSADESTUSE MEETODIL SADESTATUD Sb_2S_3 ÕHUKESED KILED

MASTER THESIS

Student: Siddharth Ashok Kumar

Student Code: 184651KAYM

Supervisor: Jako Siim Eensalu

Tallinn 2020

(*On the reverse side of title page*)

AUTHOR'S DECLARATION

Hereby I declare, that I have written this thesis independently.

No academic degree has been applied for based on this material. All works, major viewpoints and data of the other authors used in this thesis have been referenced.

"Siddharth Ashok Kumar" ....May 2020…..

Author: ....

      /signature /

Thesis is in accordance with terms and requirements

"......." .... 20….

Supervisor: Jako Slim Eensalu…............

      /signature/

Accepted for defence

"......."....................20… .

Chairman of theses defence commission: ....

      /name and signature/

Non-exclusive Licence for Publication and Reproduction of Graduation Thesis[1]

I, Siddharth Ashok Kumar_ (name of the author) (date of birth: May 14, 1990.) hereby

1. grant Tallinn University of Technology (TalTech) a non-exclusive license for my thesis

_____
_____
_____
_____,

<div align="center">(title of the graduation thesis)</div>

supervised by _____Jako Slim Eensalu_____,

<div align="center">(Supervisor's name)</div>

1.1 reproduced for the purposes of preservation and electronic publication, incl. to be entered in the digital collection of TalTech library until expiry of the term of copyright;

1.2 published via the web of TalTech, incl. to be entered in the digital collection of TalTech library until expiry of the term of copyright.

1.3 I am aware that the author also retains the rights specified in clause 1 of this license.

2. I confirm that granting the non-exclusive license does not infringe third persons' intellectual property rights, the rights arising from the Personal Data Protection Act or rights arising from other legislation.

---

[1] *Non-exclusive Licence for Publication and Reproduction of Graduation Thesis is not valid during the validity period of restriction on access, except the university`s right to reproduce the thesis only for preservation purposes.*

_____ (*signature*)

_____ (*date*)

<div align="center">Faculty of Chemical and Materials Technology</div>

THESIS TASK

Student: Siddharth Ashok Kumar, 184651KAYM (name, student code)

Study programme: Materials and Processes for Sustainable Energetics (code and title)

main speciality: Materials for Sustainable Energetics

Supervisor(s): Young Researcher, Jako Siim Eensalu, 6203369(position, name, phone)

Consultants: …………………………………………………..(name, position)

……………………………………………………………… (company, phone, e-mail)

Thesis topic:

(in English)   The topic of this research is to investigate the feasibility of producing Sb_2S_3 thin films from a metal organic precursor not previously used in spray pyrolysis.

(in Estonian) Selle uurimistöö teemaks on uurida Sb_2S_3 õhukeste kilede valmistatavust pihustussadestuses eelnevalt kasutamata metallorgaanilisest lähteainest.

Thesis main objectives:

1. Produce thin layers containing Sb by ultrasonic spray.

2. Produce thin layers containing Sb_2S_3 by ultrasonic spray.

3. Produce thin films of only Sb_2S_3 by using ultrasonic spray in air.

Thesis tasks and time schedule:

No	Task description	Deadline
1.	Find the conditions for a practically applicable spray solution.	01.02.2019
2.	Find the deposition and annealing conditions to achieve the main objectives	01.03.2020

Language: English   **Deadline for submission of thesis:** "26" May 2020

Student: ………………….   …..…..…......... "……."……….....................201….a
                               /signature/

Supervisor: …………………   ……………………..   "……."…...................201….a
                               /signature/

Consultant: …………………   …......................   "……."…...................201….a
                               /signature/

Head of study programme: ……………   .... "……."…...................201.a
                               /signature/

4

CONTENTS

PREFACE

This study was initiated by Young Researcher Jako Siim Eensalu, MSc at the Laboratory of Thin Film Chemical Technologies at Tallinn University of Technology, where the major thesis work was also done. Senior Researcher Dr. Olga Volobujeva, PhD, from the Laboratory of Optoelectronic Materials at Tallinn University of Technology measured the scanning electron microscopy and energy dispersive X-ray spectroscopy data included in this thesis. The Raman data included in this thesis was measured by Jako Siim Eensalu. Senior Researcher Dr. Ilona Oja Acik was consulted in the writing stage of this thesis.

The aim of this study is to investigate the effect of deposition and post deposition annealing conditions on the properties of deposited Sb containing layers with the ultimate goal to obtain phase pure Sb2S3 layers from the synthesis route via ultrasonic spray pyrolysis of this novel metal-organic coordination complex precursor.

The aim of this study is to investigate the effect of deposition and post deposition annealing conditions on the properties of deposited Sb containing layers with the ultimate goal t obtain phase pure Sb2S3 layers from the synthesis route via ultrasonic spray pyrolysis of this novel metal-organic coordination complex precursor. for effective utilization of time, capital and scalability, Ultrasonic Chemical spray pyrolysis was be employed. The spray solution was prepared using single source metal organic coordination complex of antimony using chlorobenzene and toluene as solvents. The deposition temperatures were 140^oC and 100^oC for chlorobenzene and toluene respectively. Annealing was carried out at 270^oC and 300^oC in flowing N_2 gas.

When chlorobenzene was used as a solvent, SEM results showed the inhomogeneous phase present in the both as-deposited and annealed samples' EDX measurements showed the oxidation of films which was later confirmed by XRD and Raman spectroscopy. The E_g for as-deposited film and annealed film was estimated to be 1.9eV and 1.54 eV. When toluene was used as solvent with dynamic nozzle movement, it was evident that 100^oC was the ideal deposition temperature since the deposition at 140^oC resulted in oxidation. Finally, with employment of static spray system, desired Sb_2S_3 film was deposited. The result was backed by XRD and Raman spectroscopy. The E_g for annealed film deposited by dynamic and static spray system was estimated to be 1.5 eV and 1.55 eV respectively.

Keywords: Antimony sulfide, thin films, ultrasonic spray pyrolysis, master thesis

Lists of abbreviation and symbols

ALD   Atomic layer deposition

CBD   Chemical bath deposition

CdTe   Cadmium telluride

CSP   Chemical spray pyrolysis

CSS   Closed space sublimation

$Cu(In,Ga)Se_2$ Copper Indium Gallium selenide

EDX   Energy-dispersive X-ray spectroscopy

E_g Band gap energy

PET   Polyethylene terephthalate

PV   Photovoltaic

SEM   Scanning electron microscope

Si   Silicon

USP   Ultrasonic spray pyrolysis

UV-VIS   Ultraviolet-Visible spectroscopy

XRD   X-ray diffraction

1. INTRODUCTION

The need for comfortable and luxurious life has catapulted human beings from nomadic hunters and gatherers to agrarians and to the modern human civilization. As our civilization moves forward in search of elusive better life, the consumption of energy is increasing in an unprecedented scale. The never ending hunger for energy has led to the exploitation of non-renewable energy sources, mainly fossil fuel. The drastic growth of human population is pushing non-renewable energy sources to the brink. The extensive use of fossil fuel has led to the manifestation of "Global is warming". To overcome or to mitigate the effects of global warming humanity is searching for alternate and sustainable renewable energy sources. One such renewable energy source is "solar energy".

The solar energy can be harnessed to a reasonable degree all around the globe and it promises a hopeful future but the use of toxic elements in compounds such as lead sulfide, Cadmium telluride(CdTe), $Cu(In,Ga)Se_2$, a major concern [1].

Antimony Sulfide (Sb_2S_3) is a non-toxic, adequately available material that can be used in the mass production of solar cells and as a result extensive research is being carried out on Sb_2S_3 based solar cells. Various thin film coating techniques such as Chemical Bath deposition, Vapour Transport deposition, Spin Coating, Chemical Vapour deposition, Thermal Evaporation, Sputtering can be employed. However for effective utilization of time and cost, Ultrasonic Chemical spray pyrolysis can be employed.

The solution was prepared using single source metal organic coordination complex of antimony using chlorobenzene and toluene as solvents. The deposition temperatures were 140^oC and 100^oC for chlorobenzene and toluene respectively. Annealing was carried out at 270^oC and 300^oC in flowing N_2. Optical microscope was used for the preliminary examination of the as-deposited and annealed films. Material characterizing techniques like scanning electron microscopy (SEM), x-ray diffraction spectroscopy (XRD), UV-VIS spectroscopy and Raman spectroscopy were employed.

2. LITERATURE REVIEW

The conversion of light energy to useful electrical energy is the basic principle behind all photovoltaic (PV) devices. Just like most of the earlier discoveries were due to lucky accidents, the discovery of photovoltaic phenomenon was also one of them. The photovoltaic effect was first discovered by French physicist, Alexandre Edmond Becquerel in 1839 [2]. In 1905 Albert Einstein published a paper on explaining the theory behind "Photovoltaic Effect" which won him a noble prize [3]. The process of generation of electricity and voltage upon the exposure of sunlight is known as photovoltaic effect. This is also the basic principle behind the working of solar cells [4].

Semiconductors are largely used in the construction of PV cells. Semi-conductors are the materials whose conductivity lies between that of conductor and insulator. Conductivity of the semiconductor can be increased by introducing impurities to its crystal structure which is called as doping and the impurities are called as dopants. Silicon is the most commonly used semiconductor since it is abundantly available [5]. Silicon has four unpaired electron in its outer most shell which makes the valency of silicon four. Below figure shows the atomic arrangement of silicon [6].
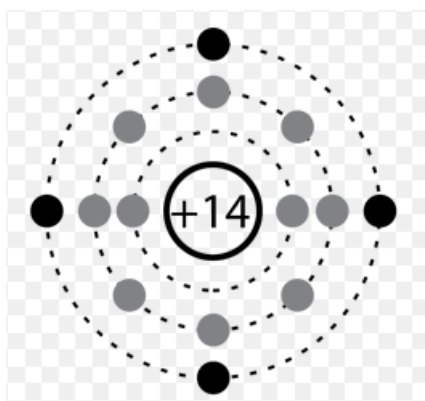
Figure 0.1 Atomic structure of Silicon (Si).

Silicon can be doped in two ways: N-type doping and P-type doping. When silicon is doped with 5 valent dopant, four outer electrons combine with ever one silicon atom, while the fifth electron is free to move and serves as charge carrier. This is called as N-type doping. This free electron requires much less energy to be lifted from the valence band into the conduction band, than the electrons which cause the intrinsic conductivity of silicon. The most commonly used 5-valent dopants are phosphorus, antimony and arsenic [7]. Figure 2 shows the N-type doped silicon [8].
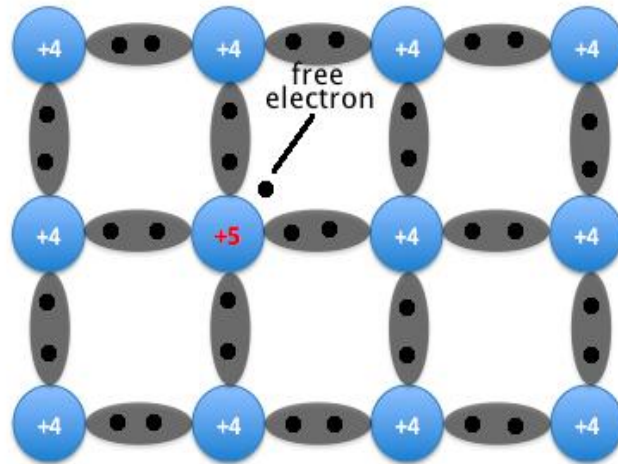
Figure 0.2 Silicon doped with 5-valent dopant

In contrast to N-type doping, when 3-valent dopant is introduced to silicon it pairs with 3 outer electrons of silicon leaving one unpaired electron which gives rise to a hole. Figure 3 shows the P-type doped silicon [8].
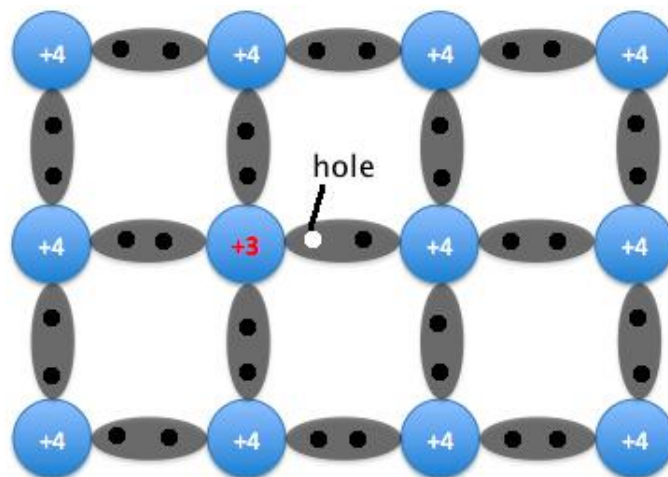
Figure 0.3. Silicon doped with 3-valent dopant

P and N type silicon are not of much use since they are electrically neutral.When P and N type silicon material are broubht together ,it give rises to PN junction. Since N-type region has high electron concentration and P-type has high hoe concentraion,electron diffuse from N-type to P-type side and holes diffuse from P-type to N-type side [9]. PV junction is the building block of solar cells.

Binary charcogenides materials have attracted attention due to their many unique electrical and optical properties [10] [11].Antimony sulfide is one among these materials. Antimony sulfide (Sb_2S_3) is an environmentally friendly material and is available abundantly on earth's crust [12].Antimony Sulfide has reported to be non-toxic and stable element [13]. Antimony sulfide has found its application in solar cells, thermoelectric devices, switching devices, microwave and television camera [14]. The crystal structure of antimony sulfide falls to the orthorhombic crystal system. Unit cell parameters of Sb_2S_3 are a=11.229Å, b=11.31Å, c=3.8389Å and the unit cell volume is 487.54 $Å^3$ [15]. Figure 4 shows the structure of Antimony Sulfide.
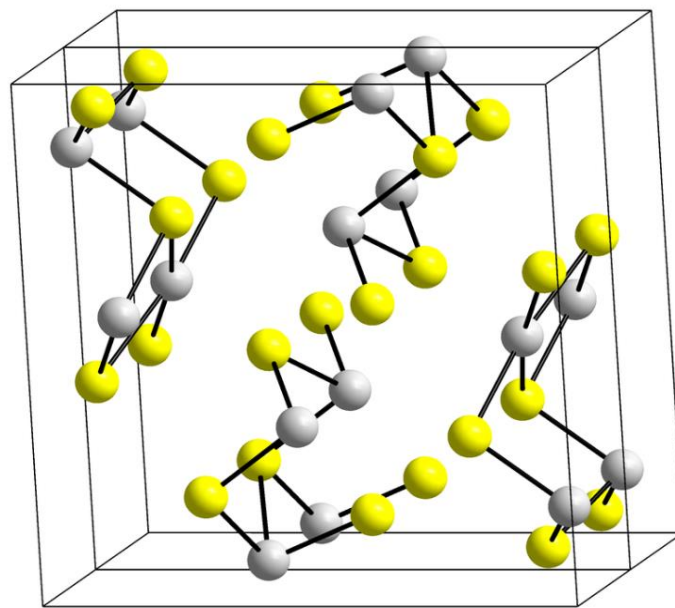
Figure 0.4 Structure of Antimony sulfide.

Both amorphous and crystalline antimony sulfide have high absorption coefficient of $1.8*10^5cm^{-1}$ and $7.5*10^4cm^{-1}$, and have direct band gap of 2.24eV and 1.73eV respectively. These optical properties have made antimony sulfide thin film a promising contender for application as solar absorber [12].

There are many deposition techniques to obtain antimony sulfide thin films such as closed space sublimation (CSS), atomic layer deposition (ALD), sputtering, electro deposition (ED), chemical bath deposition (CBD), thermal evaporation, pulse electron deposition (PED), spin coating and Chemical spray pyrolysis (CSP) [16] [17] [18]. Chemical spray pyrolysis has received considerable attention because of its simplicity and cost effectiveness, since scalability greatly depends on these parameters. Some of the advantages of CSP are mentioned as follows [19].

- Any element in the form of spray solution can be used to dope deposited films

- CSP does not require high quality targets, high quality substrates or vacuum at any stage of deposition.

- Thickness of films and their deposition rate can be easily controlled by changing spray parameters.

- CSP operates at moderate temperature (100°C-500°C).

- It does not cause the localized heating effect which can be detrimental for the deposition process.

- There are no restriction on substrate material, size and its surface profile.

- Films with composition gradient and layered films can be deposited by changing the composition of solution.

The aim of this study is to investigate the effect of deposition and post deposition annealing conditions on the properties of deposited Sb containing layers with the ultimate goal t obtain phase pure Sb_2S layers from the synthesis route via ultrasonic spray pyrolysis of this novel metal-organic coordination complex precursor

3. EXPERIMENTAL PROCEDURE

This chapter lays out the detailed description of the steps involved in the experiments conducted pertaining to this study in the laboratory of Thin Film Chemical Technologies in the department of Materials and Environmental Technology at Tallinn University of Technology. This chapter also gives brief description of the materials characterization techniques used in the study and their working principles.

3.1 Sample preparation

3.1.1 Substrate preparation

The substrate plays an important role in the outcome of the quality of films in any thin film deposition techniques. Any foreign materials like organic or inorganic residues present on the substrate may distort the orientation of the crystals in thin films and may also lead to the uneven surface coverage of film on the substrate [20]. Glass substrates brought from VWR International were used in the experiment. The dimension of the substrate was 26x76x1. The substrates were cut into 3 equal parts using a diamond tip cutting tool. Residual glass particles were blown off with a hand held air pump. Then, deionized water ($18.2 M\Omega cm^{-1}$) was used for the cleaning of substrate, followed by ethanol (96.6 vol%, Estonian spirits Ltd.) to remove any organic material present on the substrate. Residual cleaning solution droplets and dust particles were blasted off the surface of the substrate to speed up the drying process and to ensure clean substrate surface for deposition. Finally, the substrates were immersed in boiling deionized water for 40 minutes. Then, the substrates were placed on the hot plate of ultrasonic spray pyrolysis system to dry at 110^oC before the deposition process.

3.1.2 Solution preparation

A metal organic coordination complex comprising of antimony and sulphur was used as the single source precursor for the preparation of the solution. The single source precursor was prepared by my supervisor Jako Siim Eensalu in the laboratory of Thin Film Chemical Technologies. The exact composition and chemical structure of the precursor cannot be discussed since it is involved in two patent applications and it should remain classified for the same reason.

The single source precursor is composed of elements like Hydrogen, Oxygen, Carbon, Sulphur and Antimony. The ratio of Sulphur to Antimony is 6 to 1.The

precursor is light yellow in colour and it is stable when stored at room temperature. The precursor was weighted using digital analytical scale. The weighing equipment and trays were cleaned with ethanol prior to the weighing of precursor. The weighed precursor was transferred to the volumetric flask which had pre-emptively been cleaned using deionized water, alcohol and the organic solvent used in the preparation of the solution in this specific order and dried in air at 60^0C. The quantity of the organic solvent depends on the molarity of the solution used during deposition. The solvation of the precursor in the solvent was relatively slow at standard temperature and pressure. To accelerate the solvation process, a magnetic stirrer was used. The temperature of water bath was set at 40^oC, and the mixing was continued until a clear solution was obtained.

3.1.3 Deposition condition

Deposition conditions dictate the overall properties of the deposited film. There are four such major variables in ultrasonic spray pyrolysis: deposition temperature, carrier gas flow rate, nozzle distance and deposition time. It is of high importance to figure out the parameters of each variable, to find the optimum, where a film with required properties can be deposited. Since the deposition was carried out with the use of different organic solvents like ethanol, chloro-benzene and toluene, all variables had to be tweaked accordingly. The various deposition condition are tabulated below.

Table 3.1 Overview of deposition and post-deposition annealing conditions of samples that were characterized further.

Sample	Solvent	Solution Molarity mM	Deposition Temperature ^{o}C	Carrier Gas L/min	Deposition Time min	Annealing Temperature ^{o}C	Annealing Atmosphere ^{o}C
CB-AD	Chloro-Benzene	60	140	10	10	As-Dep	As-Dep
CB-AN	Chloro-benzene	60	140	10	10	300	N_2
T1-AD	Toluene	60	100	5	10	As-Dep	As-Dep
T1-AN	Toluene	60	100	5	10	300	N_2
T2-AD	Toluene	60	140	5	10	As-Dep	As-Dep
T2-AN	Toluene	60	140	5	10	300	N_2
T3-AD	Toluene	60	180	5	10	As-Dep	As-Dep
T3-AN	Toluene	60	180	5	10	300	N_2
T4-AD	Toluene	100	100	10	10	As-Dep	As-Dep
T4-AN	Toluene	100	100	10	10	270	N_2

3.1.4 Annealing condition

Tuning of annealing conditions is important to obtain the desired materials properties after heat treatment of the deposited thin film on the glass substrate. From the experimental trials it was found that the temperature above 320°C resulted in the decomposition of the film and the temperature below 150°C resulted in no crystal formation or partial crystal formation on the film. Guided by experimental trails and literature review, the annealing temperature was set at 300°C for samples CB,T1, T2 and T3. Before annealing, the furnace tube was cleaned with strong acids like sulphuric acid and hydrochloric acid, followed by washing with deionized water. The furnace tube was dried completely before inserting the samples to exclude moisture. Then, the as deposited samples were introduced into the furnace tube. Nitrogen supply tube was connected to the inlet of the furnace tube and outlet was connected to the tube which was directed toward ventilation system. Nitrogen was pumped inside the furnace tube for 15 minutes to purge the atmospheric gases since the presence of oxygen and water during the annealing process would lead to the formation of antimony oxides instead of antimony sulfide. Then, the quartz tube was placed into the furnace and heated to 300°C. The samples were annealed for five minutes, after which the film colour changed from orange yellow to grey.

3.2 CHARACTERIZATION TECHNIQUES

3.2.1 Optical Microscopy

Optical microscopy is a non-destructive technique where the results can be obtained in real time. The magnified image of an object is created by an objective lens, and this image is further magnified by a second lens system (the eyepiece) for viewing, forming an air-separated couplet. The final magnification can then be calculated as the product of the magnifying power of the objective lens times the magnifying power of the eyepiece.

The virtual image comes to a focus between the 2 lenses of the eyepiece. The first lens will bring the real image into focus, and the second lens will then enable the eye to focus on the virtual image. The magnified image of an object is created by the schematic of basic optical microscopy is shown in the figure 5 [21]. . A Zeiss, Axio Imager D2m was used in this study coupled with a camera accessory to capture magnified images of the sample surface with the proprietary AxioVision program.
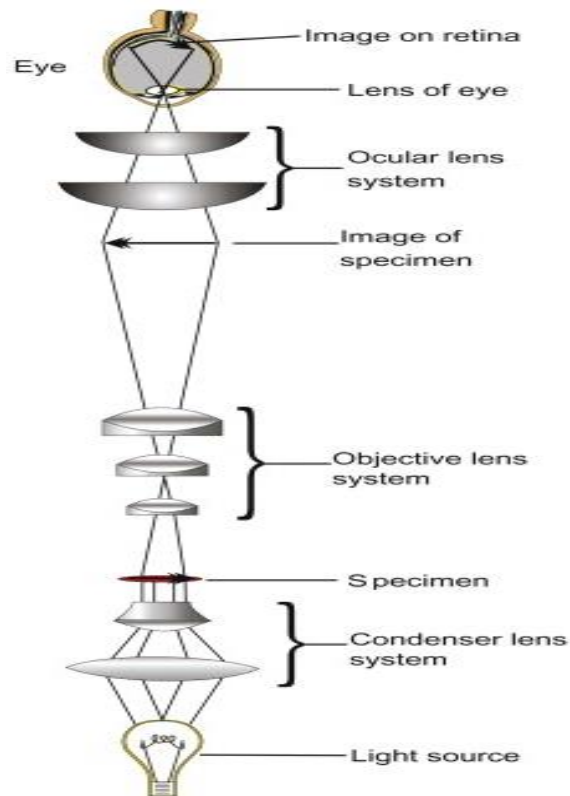
Figure 3.1 Schematic of optical microscopy

3.2.2 SEM and EDX

Scanning Electron Microscopy (SEM) is a material characterizing technique needed to study the morphology, grain size and film thickness of samples. In scanning electron microscopy, electron beams are used to gather information of the sample. When a strong beam of electron is incident on the sample, it generates secondary electron beam (SE), Back scattering electron beam (BSE) and characteristic x-rays. SE originates from the surface of the sample while BSE originates from deeper region of the sample and characteristic x-rays originate from the interaction between electron beam and matter. SE gives information on the sample morphology whereas in BSE gives information on the volumetric composition of the sample. Characteristic x-ray gives the elemental composition of the sample in Energy Dispersive X-ray Spectroscopy (EDX). Zeiss Ultra-55 SEM equipment was used for the imaging .Accelerating voltage ranged from 4KV to 20KV. Magnetron sputtering device Quorum Q150RS was used to coat the sample with 1nm thick Gold/Palladium to enhance the conductivity of the sample surface.
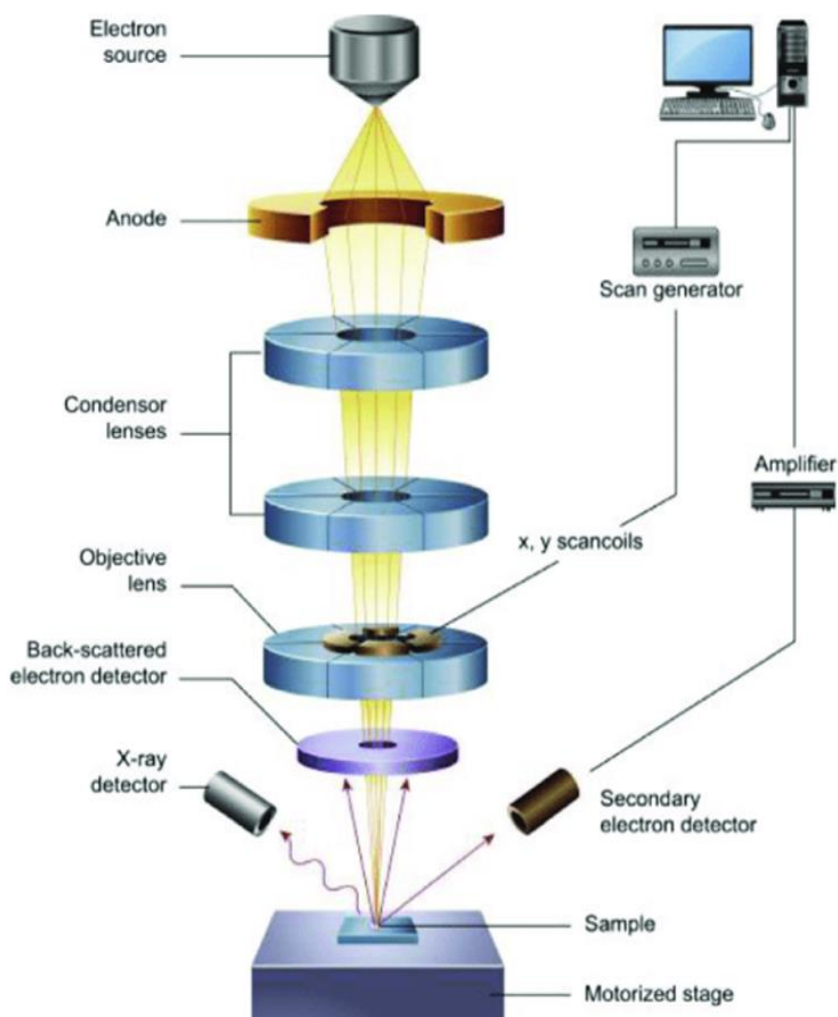
Figure 3.2 Schematics of SEM [22]

3.2.3 UV-VIS spectroscopy

UV-VIS Spectroscopy is a non-destructive, quantitative measurement of transmission or reflectance of a material as a function of wavelength. It has found its application in fields like chemistry, material science, petro-chemistry, microbiology etc [23]. When the material is incident with electromagnetic rays of various wavelengths, depending on the material part of the rays are absorbed and reaming rays are transmitted and recorded as the function if wavelength. The recorded data is converted to material's UV-VIS spectrum. Every material has it own signature UV-VIS spectrum which can used to quantify a material [24]. UV–VIS can be used to identify unknown compounds present in the sample. When the spectrum of unknown material is compared with spectrum of a reference material and if the spectrum matches, material can be successfully identified [25].IN this study the main goal for using UV-VIS technique was to calculate absorbance and

band gap of the films. Absorbance can be calculated by using equation mentioned below.

$$Ab = 100 - TR - TT$$

Where Ab stands for absorbance, TR stands for total reflectance and TT stands for total transmittance. Band gap can calculated by plotting the ahv^2 ($eVcm^{-2}$) along y-axis and photon energy (eV, $1240/\lambda$) along the x-axis.
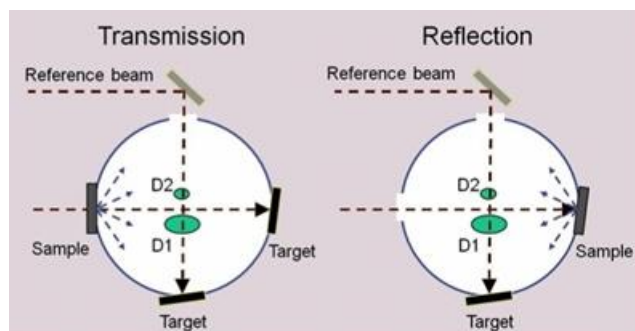
Figure 3.3 Total transmittance and Total reflectance method [8].

3.2.4 Raman spectroscopy

When a radiation of known wavelength incidents on a material, most of the radiation passes through it while a very small portion of it is scattered. The scattered radiation might be elastic or inelastic depending on its wavelength. If the scattered radiation's wavelength is as same as incident radiation's wavelength, then it is called as elastic scattering. If the scattered radiation's wavelength is not as same as incident radiation's wavelength, then it is called as inelastic scattering. Every Material (compounds and elements) has its own signature way of scattering incident radiation. HORIBA LabRAM 800HR Raman spectroscopy was used to characterise the chemical composition of the samples. Measurement was carried out in the region ranging from $50cm^{-1}$ to $4000cm^{-1}$. Two lasers can be used for the excitation at two different wavelength i.e. 633nm and 532nm. The measurement was carried out by my supervisor Jako Siim Eensalu using the 532nm green laser.
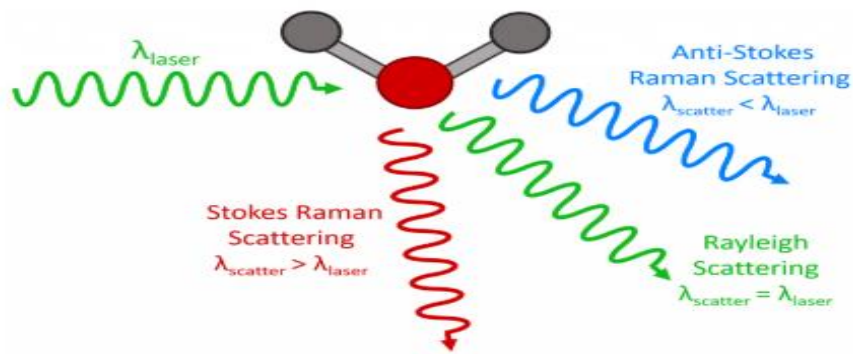
Figure 3.4 Three types of scattering [5].

3.2.5 X-Ray Diffraction (XRD)

Phase composition and crystal structure are the important aspects of thin film. X-ray diffraction (XRD) is one of the materials characterizing technique used to study the phase composition and crystal structure of thin films. It is a non-destructive method for characterizing both organic and inorganic crystalline and amorphous materials. X-rays are produced by cathode-ray tube. Initially, X-rays produced by cathode-ray tube are polychromatic in nature, which are further filtered to produce monochromatic radiation. When the monochromatic X-ray incidents on the sample, the crystal structure present in the sample diffracts x-ray in various directions. The diffracted x-ray consists of constructive interference and destructive interference. XRD analysis is based on constructive interference. The relationship between the diffraction angle and the spacing between atoms is given by Bragg's law that can be expressed in the equation i.e. $n\lambda = 2d\sin\theta$.
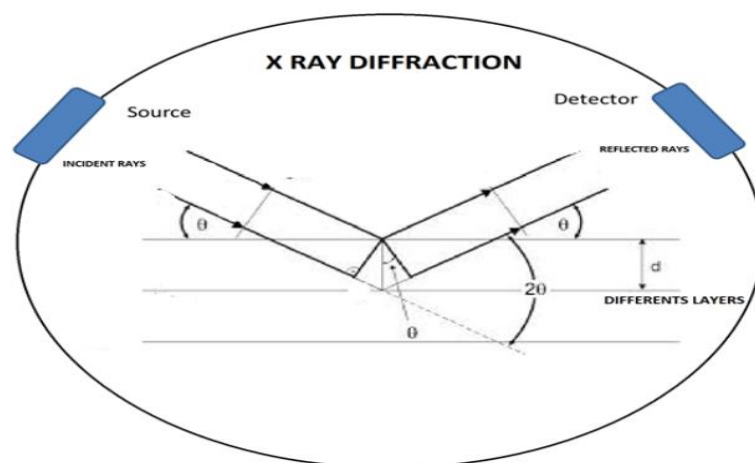
Figure 3.5 Schematics of XRD [10].

4 RESULTS AND DISCUSSION

4.1 Solution choice

Different solvents were tried for solution making in search better solubility of precursor. Water, methanol, ethanol, chloroform, chloro-benzene, and toluene were included in the experiment as potential solvents. In addition, the solvent must be liquid in standard conditions to prepare the spray solution, and gaseous slightly above or below the substrate temperature used in the deposition process, depending on the specific aim. Also, the solvent must have low viscosity, and surface tension, or the ultrasonic generator cannot generate fine droplets. Therefore, the melting point and boiling point of all solvents (Table 4.1) were screened before conducting further experiments.

The density of the solvent can affect the mass per unit time of the organic solvent reaching the substrate, which can result in carbon contamination. Density must also be considered in terms of materials usage efficiency, as about twice as much chloroform would be consumed compared to toluene in otherwise identical conditions, a matter that is not of immediate importance in this study, but must be kept in mind for future experiments and application oriented projects. Thus, the density of the solvent should also be kept in mind in terms of practical consideration.

- Water was eliminated as solvent, because the solubility of the precursor was very poor. This can be attributed to the high polarity of the water molecule since the precursor is relatively nonpolar. It is common knowledge that the polarity of solvent and solute should be relatively similar to obtain clear solution, i.e. practically useful solubility.

- Methanol was eliminated as solvent since the solubility was very poor (<5 mM), and the precursor decomposed over time, as the colour of the solution darkened immediately. A red precipitate formed in less than 10 minutes. After less than a week, a red film formed on the wetted walls of the glass.

- Ethanol was eliminated as solvent since the solubility of the precursor was poor (<10 mM), and a white precipitate formed in less than an hour. After a month of storage, a yellow film formed on the wetted walls of the glass vial. Ethanol was eliminated as solvent since the solubility of the precursor was poor, leaving a white precipitate.

- Solubility in chloroform was significantly higher, over 60 mM, which is in principle suitable for use in deposition. Chloroform was eliminated as solvent since it dissolved the polyethylene tereftalate (PET) film separating the solution from the cooling water inside the ultrasonic generator tank during operation. Without ultrasonic oscillation, the solvation of the PET membrane is considerably slower, as the membrane was intact after being submerged for 15 minutes in chloroform at standard conditions. Chloroform caused structural disintegration of the PET film in less than a minute of ultrasonic oscillation during operation, which is unacceptable for use in the experiment [29].

- Chlorobenzene dissolved over 60 mM of the precursor, and toluene dissolved over 100 mM of the precursor in pilot tests after thorough mixing for 15 minutes at room temperature. No precipitation was observed in the timespan of preparing the solution until the end of the deposition, i.e. 3-4 hours. Neither solvent had any effect on the PET membrane used in the ultrasonic spray generator tank. Based on this, the suitability of chlorobenzene and toluene for depositing Sb_2S_3 thin films from the precursor by ultrasonic spray was evaluated in more detail in the next chapters.

Table 4.1 List of solvents used in this study and the respective properties [30] [11]

Solvent	Chemical Formula	Structure	Boiling point°C	Melting point°C	Density (g/mL)	Viscosity (cp,20°C)	Relative Polarity	Toxicity
Water	H_2O		100	0	0.998	1	1	NONE
Methanol	CH_3OH		64.6	-98	0.791	0.55	0.762	H225, H301, H311, H331, H370
Ethanol	C_2H_5OH		78.5	-114	0.789	1.1(25)	0.652	H225
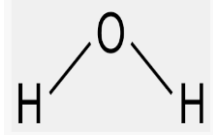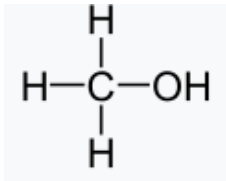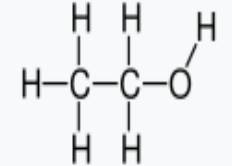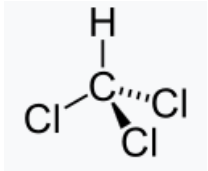
Chloroform	CHCl$_3$		61.2	-64	1.498	0.58	0.259	H302, H315, H319, H331, H351, H361d, H372
Chloro-benzene	C$_6$H$_5$Cl		132	-45	1.106	0.8	0.188	H226, H315, H332, H411
Toluene	C$_7$H$_8$		110.6	-93	0.867	0.59	0.099	H225, H304, H315, H336, H361d, H373
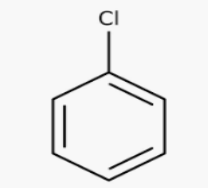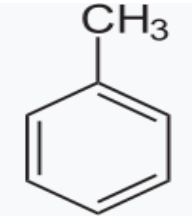
GHS hazard codes used in the able are explained below.

- H225:Highly flammable

- H301:Toxic if swallowed

- H311:Toxic in contact with skin

- H331:Toxic if inhaled

- H370: Causes damage to organ

- H302:Harmful if swallowed

- H315:Causes skin irritation

- H319:Causes serious eye irritation

- H351:Suspected to cause cancer

- H361d:Suspected to damage unborn child

- H372: Causes damage to organ through prolonged and repeated exposure.

- H226:Flamable liquid

- H332:Harmful if inhaled

- H411:Toxic to aquatic life with long lasting effect

- H304:May be fatal if swallowed and enters airway

- H336:May causes drowsiness and dizziness

- H373: May cause damage to organ through prolonged and repeated exposure

4.2 Effect of Chlorobenzene on film properties

4.2.1 Optical microscopy study on as deposited and annealed films

Optical microscopy was used to investigate the quality and homogeneity of the prepared thin films. Figure 4.1 show the surface of the film deposited at 140°C using chlorobenzene as solvent. Figure 4.1A shows the as deposited film while the figure 4.1B shows the film annealed at 300°C.It can be observed from the figure 4.1A that the as-deposited film is highly porous in nature and the uneven distribution of the film is evident. From figure 4.1B, the presence of inhomogeneous film can be observed. Seeing as there was no film or layer definitely present, further investigation was carried out using SEM.
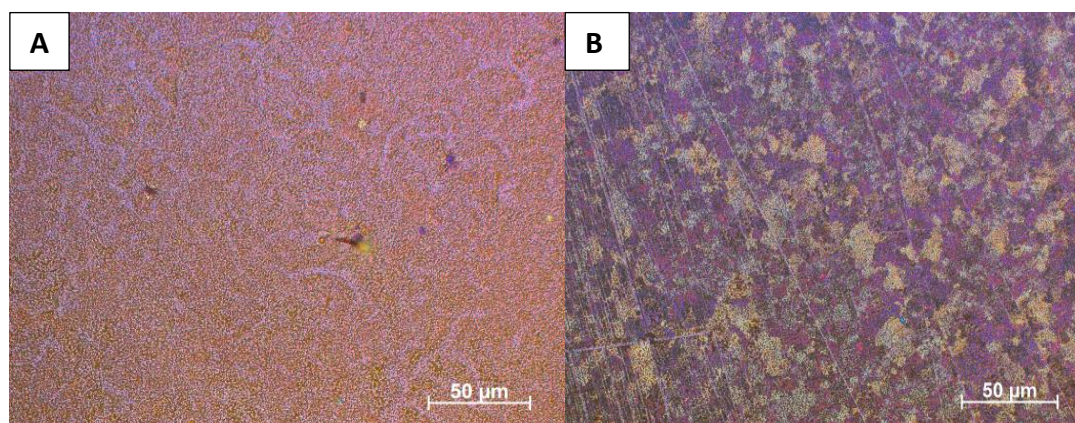
Figure 4.1 Surface views in polarized transmittance mode, by optical microscopy, of the as deposited film, deposited at 140°C (A), and the film annealed at 300°C in flowing N$_2$ (B). Substrate: soda lime glass

4.2.2 Morphology of as deposited and annealed films by SEM study

SEM was used to study the surface morphology and cross-section of as deposited and annealed films, deposited at 140°C and annealed at 300°C, respectively, using chlorobenzene as the solvent. Figure 4.2A and figure 4.2B shows the morphology of as deposited and the annealed film. SEM images agree with the optical microscopy images on the non-homogeneity of the film. The as-deposited film contains rounded formless areas intertwined with jagged grains, which means the film is inhomogeneous. Figure 4.2B shows the morphology of the annealed film, wherein Grain boundaries were well defined and no formless round regions are observed. Although the film is still –inhomogeneous in surface morphology, as grain between 100-1000nm in lateral diameter are dotted with smaller grains or nano-rods, as will become apparent in Figure 4.2D of 50 nm in diameter. Figure 4.2C shows the cross-

sectional image of the as deposited film, where it can be observed that the adhesion between the film and the glass substrate is good since there is no evidence of edge peeling. The film is for the most part dense throughout its thickness of some 400-500 nm depending on the location. Hilly morphology and vertical grain boundaries can be observed. The presence of warped nano rod or in some instances nano-banana like shapes of some 50-100 nm in diameter, and from 500 to over 1000 nm in length can be observed in Figure 4.2D which was unexpected, but otherwise typical for certain deposition conditions in films grown by USP for several metal chalcogenides, as our previous experience has shown [31] . The thickness of the annealed film was found to be 440-550nm. Further EDX analysis revealed that the atomic ratio of S:Sb was 0.37, O:Sb was 0.68 and O:S was 1.9 in the as-deposited film, indicating that the majority of the thin film could be composed of antimony trioxide, as will be confirmed by XRD in the next chapter. EDX of the annealed sample showed similar results, as the atomic ratio of S:Sb was 0.37, O:Sb was 0.57, and O:S was 1.5. The oxidation can be attributed to the high deposition temperature and prolonged exposure to the air atmosphere.
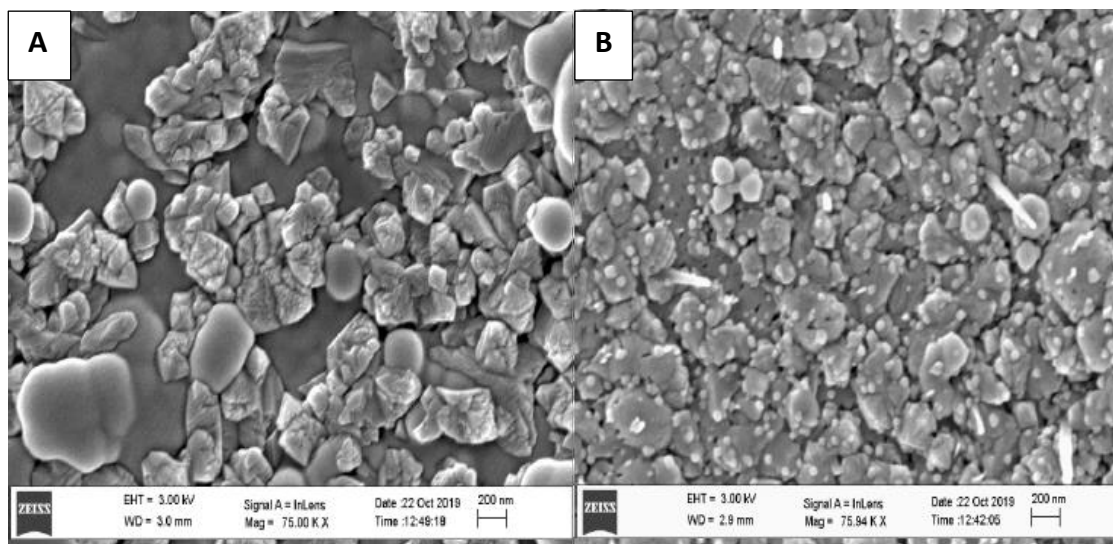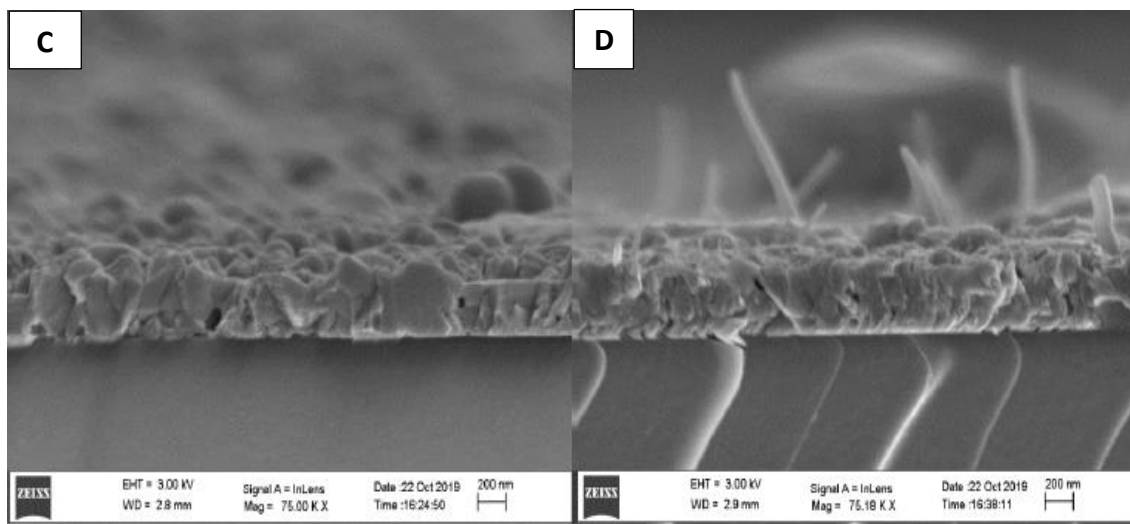
Figure 4.2 Surface, and cross sectional views, by SEM, of the as-deposited sample (a, c) deposited at 140°C from 60 mM precursor dissolved in chlorobenzene, and the of sample annealed after deposition at 300°C in flowing N2, respectively.

4.2.3 Structural properties of as deposited and annealed films deposited from chlorobenzene by XRD study

To complement the results obtained from EDX analysis, XRD was performed on the as-deposited sample deposited at $140^{o}C$ and the annealed sample deposited at $140^{o}C$ and annealed at $300^{o}C$ in flowing N_2. Figure 4.3 shows the XRD pattern of both the as deposited and annealed sample. Peaks at 13.65^{o}, 27.46^{o}, 31.86^{o}, 34.75^{o}, 45.61^{o}, 54.10^{o} are present in both of as deposited and annealed film. The main diffraction peaks matched senarmontite-Sb2O3 (ICDD PDF 00-042-1466). It can be observed from the figure that the XRD pattern of as deposited and annealed film is similar, although weak reflections of orthorhombic Sb_2S_3 (ICDD PDF 01-075-4012) are detected in only the annealed sample. The centre positions of these peaks were in agreement with the peaks of the senarmontite reference file, the thermodynamically most stable form of the trivalent antimony oxide at temperatures between 20°C and 300°C [12].
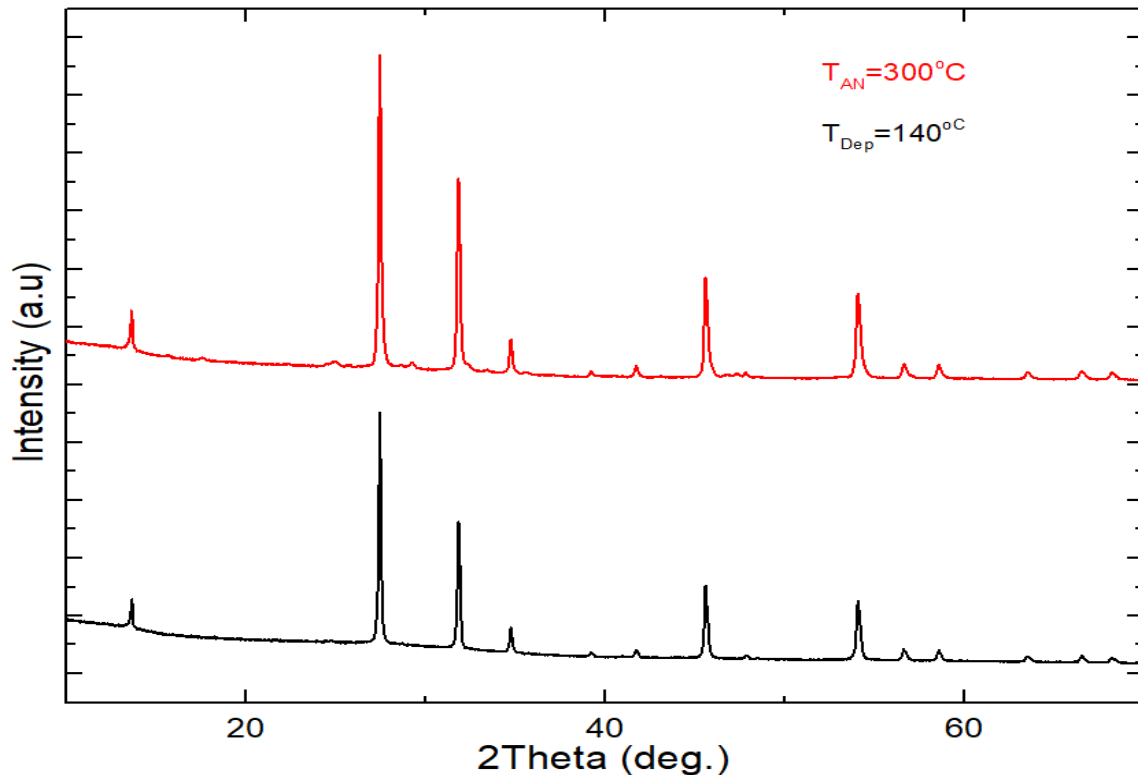
Figure 4.3 X-ray diffraction patterns of the as-deposited sample deposited at 140oC from the chlorobenzene based solution, and the annealed sample deposited at 140°C from the chlorobenzene based solution, and annealed at 300°C in flowing N_2.

4.2.4 Vibrational properties of as deposited and annealed films deposited from chlorobenzene as solvent by Raman Spectroscopy study

Raman spectroscopy study was also included to support the results obtained by XRD, and to investigate the possible amorphous phases, which XRD is not specifically meant to probe. The peak centred at 290 cm^{-1} in the as-deposited Raman spectrum of the as-deposited sample (Figure 4.4) are not well defined due to the amorphous characteristic of the film, although it is similar to previous results regarding amorphous Sb_2S_3 observed in [33] [12]. The sharp band centred at 189 cm^{-1}, 255 cm^{-1}, and 451 cm^{-1} correspond to senarmontite found in the database [32]. The vibrational bands appearing at 127 cm^{-1}, 157 cm^{-1}, 283 cm^{-1} and 300 cm^{-1} in addition to those of senarmontite in the Raman spectrum of the annealed film belong to orthorhombic Sb_2S_3, as also observed in previous studies in [33].
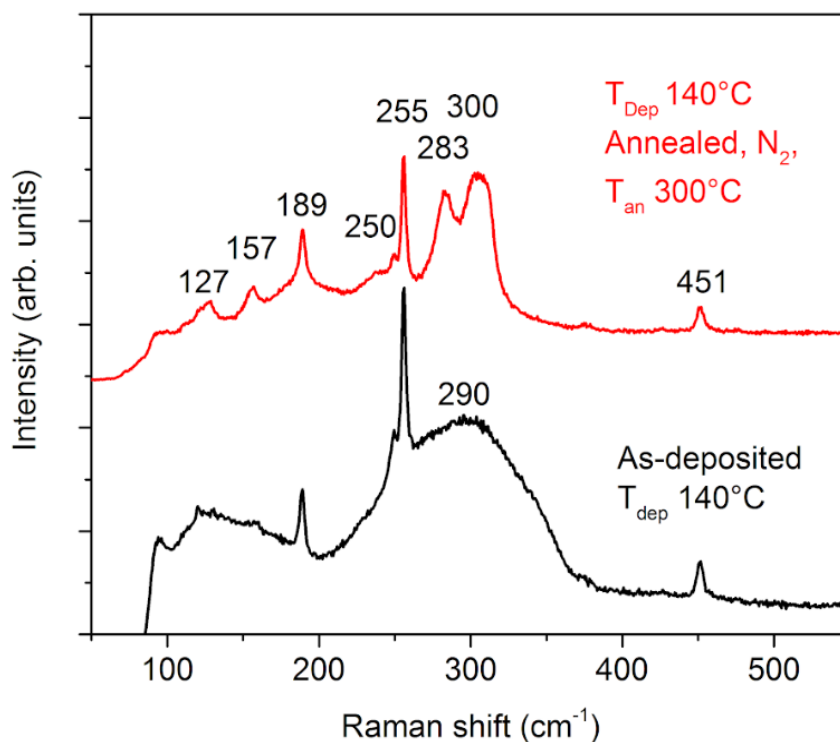
Figure 4.4 Raman spectra of film deposited at 140°C using chlorobenzene as solvent and annealed at 300°C.

4.2.5 UV-VIS spectroscopy study on as deposited and annealed films.

Total transmittance and total reflectance were measured using UV-VIS spectroscopy of both as deposited sample at 140°C and annealed sample deposited at 140°C and annealed at 300°C. Figure 4.5A shows the Total transmittance of both film and figure 4.5B show the total reflectance of both film. Absorptance of the both films was calculated, as shown in figure 4.5C. It is evident from figure 4.5C that the absorptance of the as deposited film was significantly lower in the studied wavelength region, which can be attributed to the amorphous nature of the film [12] . The band gap was calculated for the as-deposited and the annealed sample and it was estimated to be 1.9 eV for the as-deposited film and 1.54eV for the annealed film.
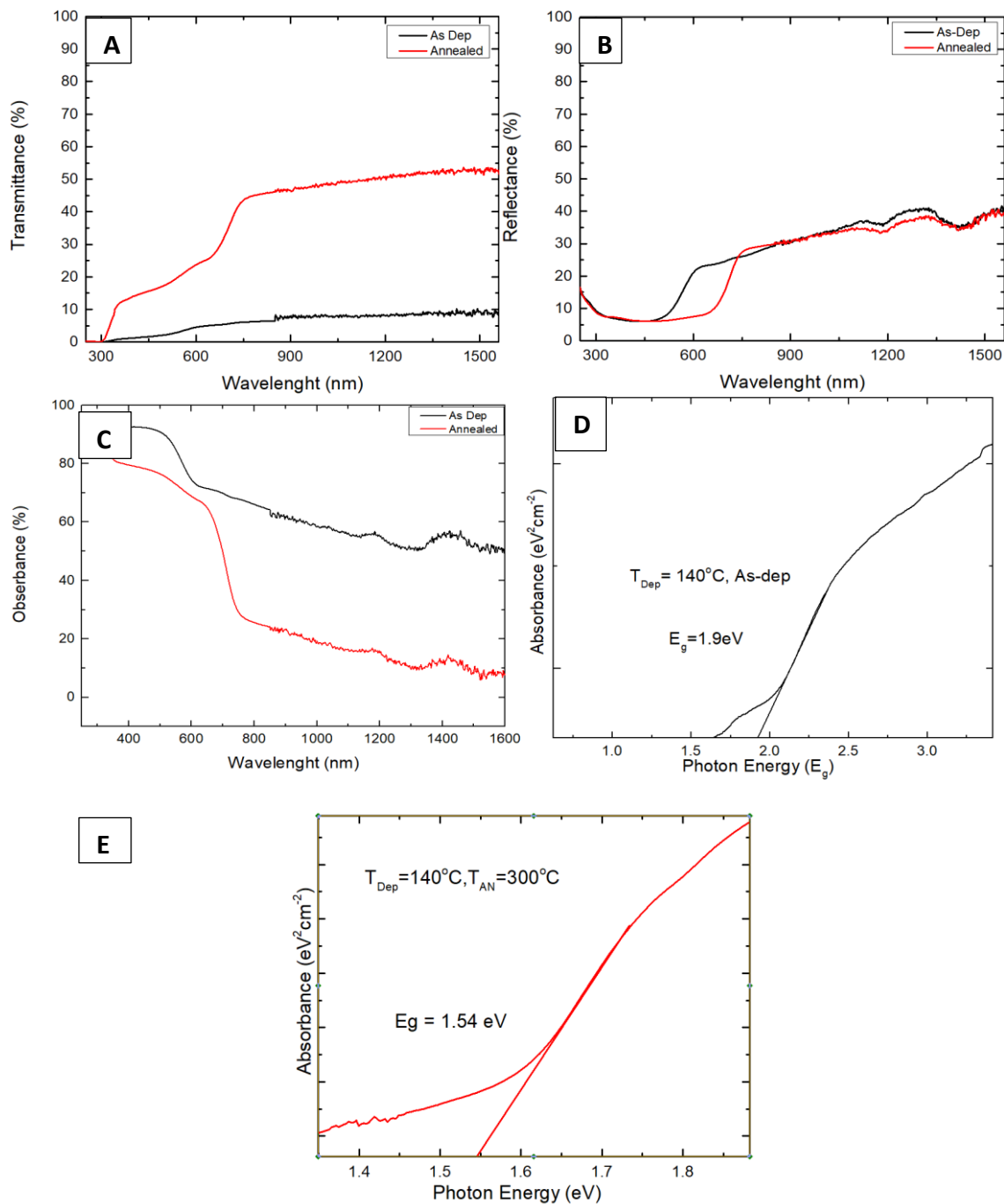
Figure 4.5 Total transmittance (A), total reflectance (B), absorptance (C), and Tauc plot (D and E) of the as-deposited sample, and the annealed (300°C, flowing N2) sample.

4.3 Effect of Toluene on film properties

4.3.1 Optical microscopy study on as deposited and annealed films

Optical microscopy was used for the preliminary inspection of the films. Figure 4.6A and figure 4.6B shows the as deposited film at 100°C and film annealed at 300°C

respectively, deposited in dynamic nozzle mode using 60mM solutions, while the figure 4.6C and figure 4.6D show the as-deposited film at 100°C and the film annealed at 270°C respectively using 100mM solution. From 4.6A and 4.6C it can be observed that the surface coverage is greater in (4.6C), and the same tendency can also be observed in annealed films (4.6B) and (4.6D). The better surface coverage and presence of less porous film can be attributed to the higher concentration of the solution and lower deposition temperature.
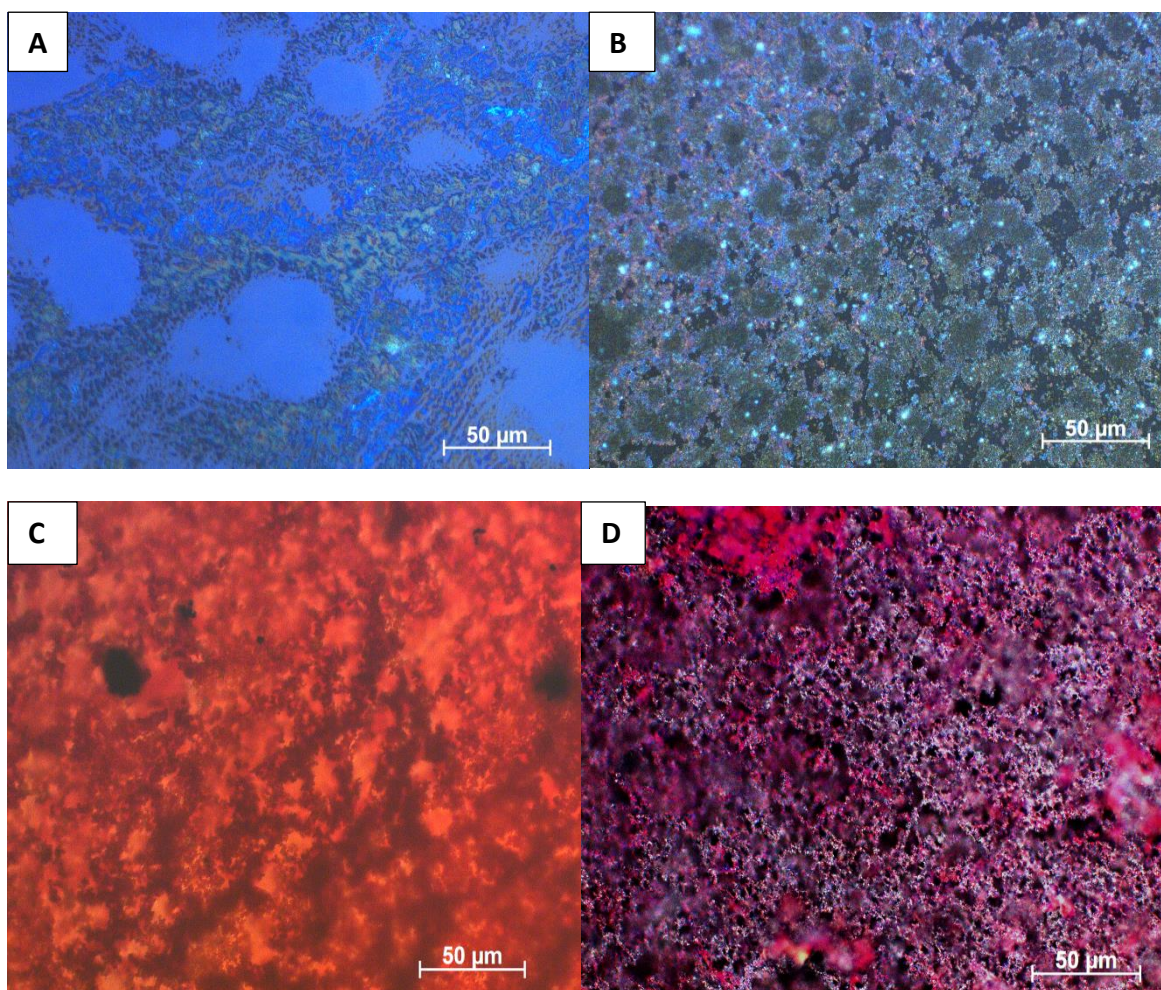
Figure 4.6 Optical microscopy image of film deposited at 100°C (A) and annealed at 300°C (B) using 60mM solution in dynamic nozzle mode respectively. optical microscopy images of film deposited at 100°C and annealed at 270°C using 100mM solution in static nozzle mode respectively.

4.3.2 Structural properties of as deposited and annealed films deposited from Toluene by XRD study

SEM was not available due to technical issue; therefore, that characterization is skipped for the following sample. XRD was performed on the as-deposited samples deposited at 100°C with 60 mM and 100 mM solution, and the annealed samples deposited at 100°C with 60 mM and 100 mM solution, followed by annealed at 300° C

and 270°C in flowing N_2. Figure 4.7A, no peaks were recorded in XRD pattern (in black, Figure 4.7 A) of as deposited film at 140°C which is due to the amorphous nature of sample. XRD pattern (in blue, figure 4.7 A) of annealed film deposited at 140°C showed peaks which were corresponding to senarmontite [31].Figure 4.7B shows the XRD pattern of film deposited at 100°C and annealed at 270°C . The diffraction peaks were analysed with respect to. The reference file ICDD PDF 01-075-4012.The peaks at 15.6°, 17.5°, 24.8°, 29.2°, 32.3°, 33.4°, 35.4° were the characteristic peaks of orthorhombic stibnite which is also known as antimony sulfide.
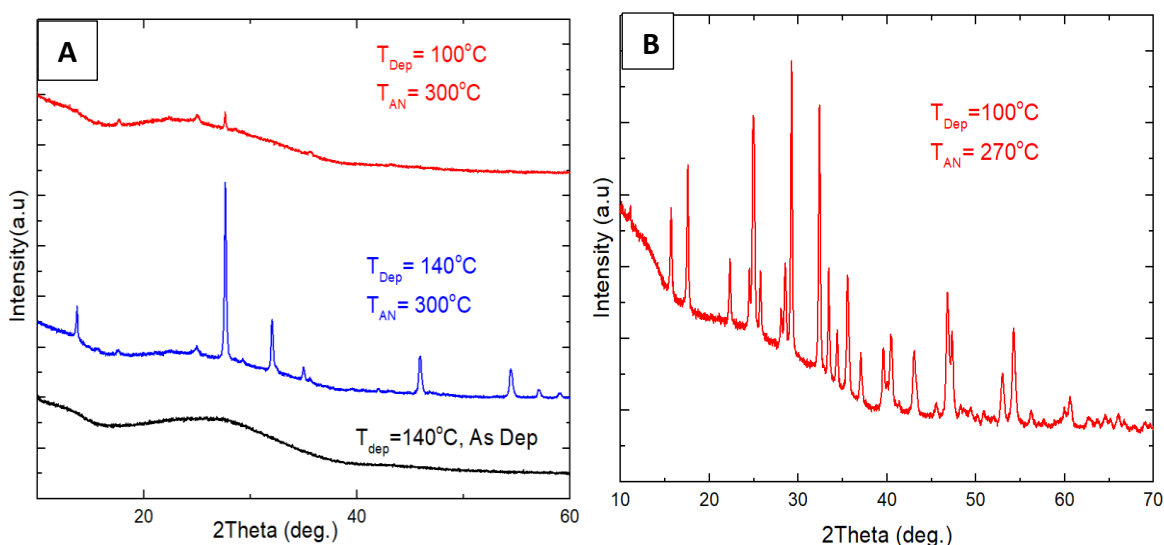
Figure 4.7 XRD patterns of as-deposited and annealed films deposited at 100°C and 140°C,followed by annealing at 300°C in flowing N_2.

4.3.3 Vibrational properties of as-deposited and annealed films deposited from toluene as solvent by Raman Spectroscopy

Raman spectroscopy was included to support the results obtained from XRD. The band centres of as-deposited sample deposited at 100°C (Figure 4.8A, Black colour) are positioned at 233cm^{-1},342cm^{-1},413cm^{-1}and 441cm^{-1} which does not match any bands of known phases of Sb_2O_3 nor Sb_2S_3. The band centers of the sample deposited at 100°C and annealed at 300°C in flowing N_2(Figure 4.8A,Red colour) are centred at 189 cm^{-1},255 cm^{-1} ,283 cm^{-1} and 451 cm^{-1}corresponding to senarmontite in the database [12] [34] and the vibrational bands centered at 157 cm^{-1}, 283 cm^{-1}, 300 cm^{-1} and

310 cm^{-1} in addition to those of senarmontite in the Raman spectrum of annealed film belong to orthorhombic Sb_2S_3 [12] [34].

The multitude of vibrational bands appearing centered at e.g. 233 cm 1, and 342 cm-1 in the Raman spectrum of the sample deposited in static nozzle mode at 100°C belong to the metal-organic coordination complex precursor, and do not overlap with Raman bands of Sb_2O_3 nor Sb_2S_3. The Raman spectrum of the sample deposited in static nozzle mode at 100°C, followed by annealing at 160°C in flowing N2 contains two broad bands, the larger one being centered at 290 cm-1, characteristic to the vibrations attributed to amorphous Sb_2S_3 [12]. The vibrational bands appearing centered at 149 cm^{-1}, 281 cm^{-1} and 300 cm^{-1} (Figure 17B, blue colour) in the Raman spectrum of the sample deposited at 100°C and annealed at 270°C in flowing N2 belongs to orthorhombic Sb_2S_3.
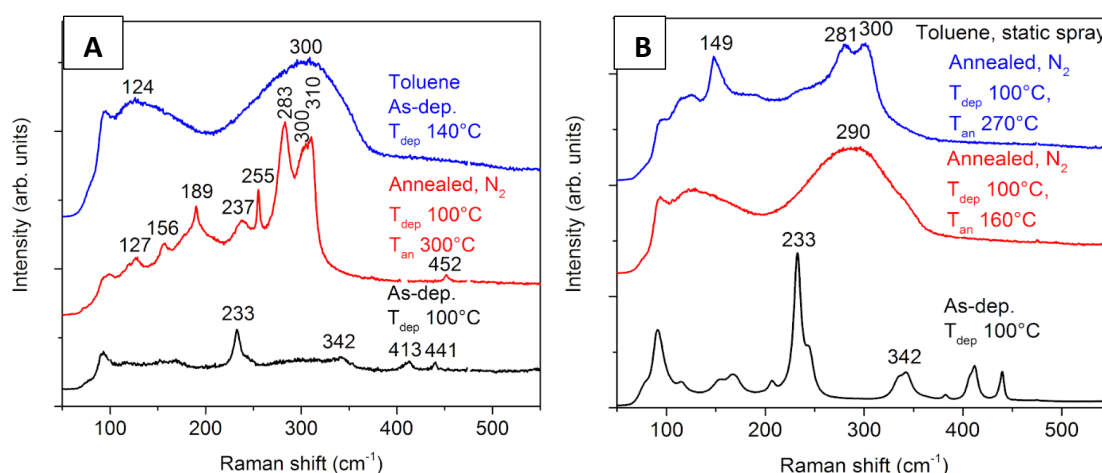
Figure 4.8 Raman spectra of as-deposited films deposited in dynamic nozzle mode at 100°C, and 140°C, and films annealed at 300°C in flowing N2 after deposition at 100°C (A). Raman spectra of as-deposited film deposited in static nozzle mode at 100oC, followed by annealing at 160°C, or at 270°C in flowing N2 (B).

4.3.4 UV-VIS spectroscopy study on as deposited and annealed films

Total transmittance and total reflectance were measured using UV-VIS spectroscopy for films deposited from 60mM solution in dynamic nozzle mode and 100mM solution in static nozzle mode, followed by annealing at 300°C or 270°C in flowing N_2, respectively. Figure 4.9A and Figure 4.9B shows the Total transmittance and total reflectance spectra respectively. Figure 4.9C shows the absorptance plot for these same. In figure 4.9C it can be observed that the absorbance of film deposited using 100mM solution is higher which can be attributed to higher thickness of film. Figure 4.9D and 4.9E shows the band gap estimation for both the film. Band gap for the film deposited using 60mM was estimated to 1.55eV and the band gap for the film deposited using 100mM was estimated to 1.5eV both of which are about 0.1-0.2 eV lower than values observed in literature [12] . This could be due to thin film interference distorting the Tauc plot, despite taking into account reflectance in the calculation. Another possible reason could be that the material is highly crystalline, resulting in close to theoretical band gap values.
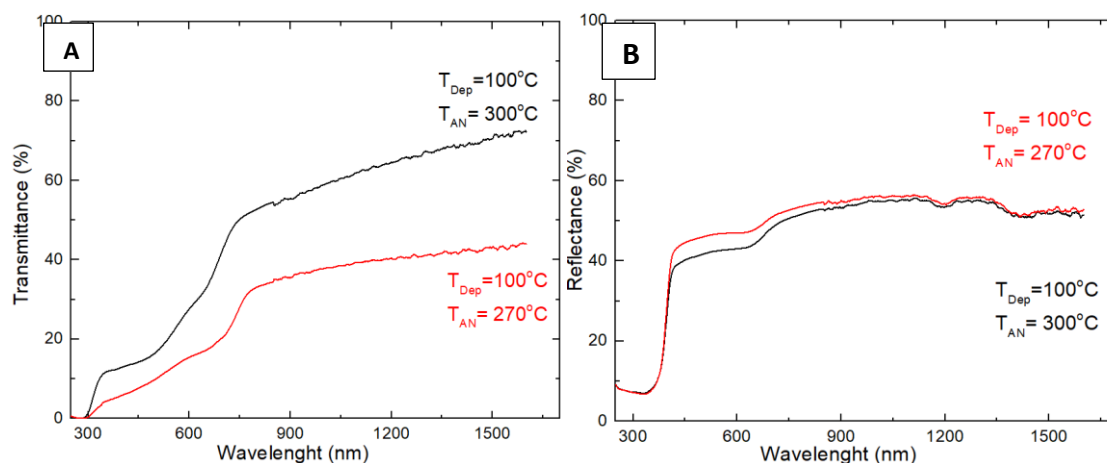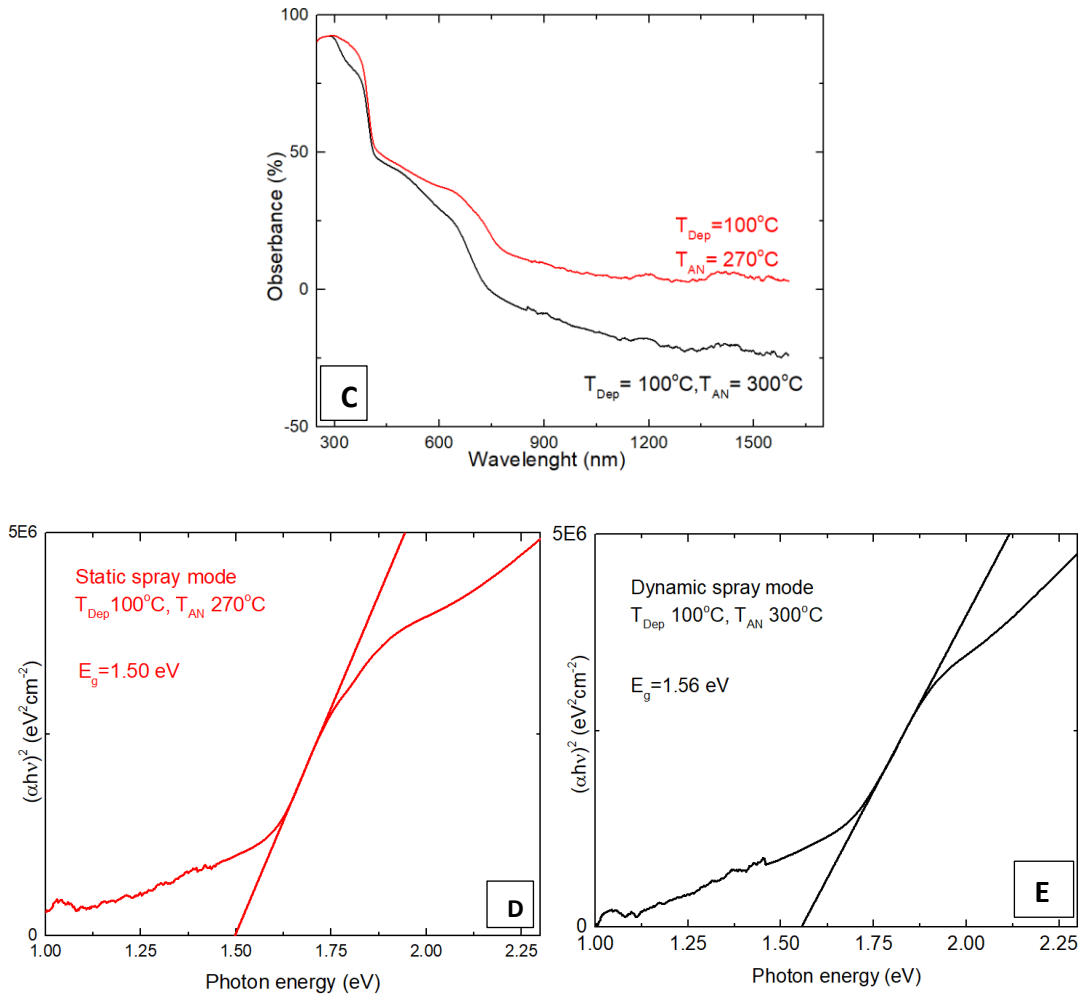
Figure 4.9 Total transmittance (A), total reflectance (B), absorptance (C), and Tauc plots (D) of the film deposited from 60 mM solution in dynamic nozzle mode, followed by annealing at 300°C, and of the film deposited from 100 mM solution in static nozzle mode, followed by annealing at 270°C in flowing N2.

5 SUMMARY

Antimony Sulphide (Sb$_2$S$_3$) is a non-toxic, adequately available material that can be used in the mass production of solar cells and as a result extensive research is being carried out on Sb$_2$S$_3$ based solar cells. Various thin film coating techniques such as Chemical Bath deposition, Vapour Transport deposition, Spin Coating, Chemical Vapour deposition, Thermal Evaporation, Sputtering can be employed. However, for effective utilization of time, capital and scalability, Ultrasonic Chemical spray pyrolysis can be employed. The spray solution was prepared using single source metal organic coordination complex of antimony using chlorobenzene and toluene as solvents. The deposition temperatures were 140°C and 100°C for chlorobenzene and toluene respectively. Annealing was carried out at 270°C and 300°C in flowing N$_2$ gas.

Optical microscope was used for the preliminary examination of the as-deposited and annealed films. Material characterizing techniques like scanning electron microscopy (SEM), x-ray diffraction spectroscopy (XRD), UV-VIS spectroscopy and Raman spectroscopy was employed. When chlorobenzene was used as a solvent, SEM results showed the inhomogeneous phase present in the both as-deposited and annealed samples' EDX measurements showed the oxidation of films which was later confirmed by XRD and Raman spectroscopy. This resulted was attributed to the higher deposition temperature and prolonged exposure to air atmosphere. The E$_g$ for as-deposited film and annealed film was estimated to be 1.9eV and 1.54 eV

When toluene was used as solvent with dynamic nozzle movement, it was evident that 100°C was the ideal deposition temperature since the deposition at 140°C resulted in oxidation. Finally, with employment of static spray system, desired Sb$_2$S$_3$ film was deposited. The result was backed by XRD and Raman spectroscopy. The E$_g$ for annealed film deposited by dynamic and static spray system was estimated to be 1.5 eV and 1.55 eV respectively.

Reference

[1] A. l. o. o. p. L. J. P. E. R. E. M. C. D.Moskowitzc, "Toxicology and Applied Pharmacology," *ScienceDirect,* vol. 147, no. 2, pp. 399-410, 1997.

[2] "pvresources.com," PVRESOURCES, 23rd Decebmer 2015. [Online]. Available: http://www.pvresources.com/en/introduction/history.php. [Accessed 22nd May 2020].

[3] "Sunlightelectric.com," sunlightelectric, [Online]. Available: http://www.sunlightelectric.com/pvhistory.php. [Accessed May 2020].

[4] G. Boyle, in *Renewable Energy: Power for a Sustainable Future*, Oxford, UK, Oxford University Press, 2004.

[5] J. Lesurf, "www.st-andrews.ac.uk," [Online]. Available: https://www.st-andrews.ac.uk/~www_pa/Scots_Guide/info/comp/conduct/semicond/semimat/semimat.htm. [Accessed May 2020].

[6] "hyperphysics.phy," [Online]. Available: http://hyperphysics.phy-astr.gsu.edu/hbase/Solids/sili.html. [Accessed May 2020].

[7] "www.halbleiter.org," [Online]. Available: https://www.halbleiter.org/en/fundamentals/doping/. [Accessed May 2020].

[8] "eng.libretexts.org," EnginneringLibreTexts, 18th May 2018. [Online]. Available: https://eng.libretexts.org/Bookshelves/Materials_Science/Supplemental_Modules_(Materials_Science)/Solar_Basics/D._P-N_Junction_Diodes/I._P-Type%2C_N-Type_Semiconductors. [Accessed May 2020].

[9] S. b. Christiana Honsberg, "www.pveducation.org," PVeducation, 2019. [Online]. Available: https://www.pveducation.org/pvcdrom/pn-junctions/formation-of-a-pn-junction. [Accessed May 2020].

[10] K. O. Savadogo, "Studies on new chemically deposited photoconducting antimony trisulfide thin films," *Solar Energy Materials and Solar Cells,* vol. 26, no. 1-2, pp. 117-136, 1992.

[11] B.B.NayakH.N.AcharyaG.B.MitraB.K.Mathur, "Structural characterization of Bi2−xSbxS3 films prepared by the dip-dry method," *Thin Solid Films,* vol. 105, no. 1, pp. 17-24, 1983.

[12] A. K. E. K. I. O. A. A. M. Jako S. Eensalu*, "Uniform Sb2S3 optical coatings by chemical spray method," *BEILSTEIN Journal Of Nanotechnology,* vol. 10, pp. 198-210, 2019.

[13] A. H. A. N. W. S. S. A. M. A. N. Ali, "Antimony sulfide, an absorber layer for solar cell application," *Applied Physics A,* 2015.

[14] M. ,. M. ,. P. Ghulam Murtaza, "Aerosol assisted chemical vapor epositionof Sb2S3 thin films," *MaterialsScienceinSemiconductorProcessing,* vol. 40, pp. 643-649, 2015.

[15] "www.mindat.org," mindat, [Online]. Available: https://www.mindat.org/min-3782.html.

[16] C. ,. M. ,. F. ,. N. R.G.AvilezGarcia, "Antimonysulfide (Sb2S3) thin films bypulseelectrodeposition," *MaterialsScienceinSemiconductorProcessing,* pp. 91-100, 2016.

[17] B. K. a. T. K. Pascal Kaienburg, "Spin-coated planar Sb2S3 hybrid solar cells,"

BEILLSTEIN Journal Of Nanotechnology, pp. 2114-2124, 2018.

[18] J. H. H. L. K. S. Y. L. M. J. Chunhui Gaoa, "Fabrication of Sb2S3 thin films by sputtering and post-annealing for solar," *Ceramics International,* 2019.

[19] P. S. Patil, "Versatility of chemical spray pyrolysis technique," *Materials Chemistry and Physics,* pp. 185-198, 1999.

[20] "dentonvacuum.com," dentonvacuum, 26 september 2019. [Online]. Available: https://www.dentonvacuum.com/what-is-pre-cleaning-in-thin-film-deposition/. [Accessed 22 5 2020].

[21] I. L. P. Timberley M. Roane, "Microscopic Techniques," in *Environmental Microbiology*, ScienceDirect, 2015, pp. 177-193.

[22] "liberaldictionary.com," [Online]. Available: https://www.liberaldictionary.com/scanning-electron-microscope/.

[23] "edinst.com," EdinburghInstruents, [Online]. Available: https://www.edinst.com/techniques/uv-vis-spectroscopy/.

[24] C. A. D. Caro, UV/VIS Spectrophotometry - Fundamentals and Applications, Mettler-Toledo , 2015.

[25] A. Choudhary, "medium.com," Medium, 12 october 2017. [Online]. Available: https://medium.com/@ankur1857/principle-of-ultra-violet-uv-spectrophotometer-e6a1c435d258. [Accessed 2020].

[26] "azonano.com," azonano, 15 july 2013. [Online]. Available: https://www.azonano.com/article.aspx?ArticleID=3554. [Accessed 2020].

[27] "edinst.com," Edinburgh Instruments, [Online]. Available: https://www.edinst.com/blog/what-is-raman-spectroscopy/. [Accessed 5 2020].

[28] "researchgate.net," ResearchGate, Jan 2018. [Online]. Available: https://www.researchgate.net/figure/Schematic-diagram-of-the-technique-of-X-ray-diffraction_fig10_323318023. [Accessed may 2020].

[29] "Miller's Home," [Online]. Available: https://sites.google.com/site/miller00828/in/solvent-polarity-table. [Accessed 15 4 2020].

[30] "PubChem," National Center for Biotechnology Information, [Online]. Available: https://pubchem.ncbi.nlm.nih.gov/. [Accessed 21 5 2020].

[31] "RRUFF," [Online]. Available: https://rruff.info/Senarmontite/R060075.

L. S. Sterling, The Art of Agent-Oriented Modeling, London: The MIT Press, 2009.